

Experimental Demonstration of Composite-Packet-Switched WDM Network

Misha Boroditsky, Nicholas J. Frigo, *Member, IEEE*, Cedric F. Lam, *Member, IEEE*, Kevin F. Dreyer, David A. Ackerman, *Member, IEEE*, John E. Johnson, *Member, IEEE*, Leonard J. P. Ketelsen, Antao Chen, and Aleksandra Smiljanić

Abstract—We propose and demonstrate experimentally a novel technique for packet switching on a ring network. We use the wavelength dimension to increase the transmission line rate and a novel packet-stacking technique to add/drop packets. Packet stacking is used for transport rate multiplication and for equal loading of wavelengths on the physical layer. Packet stacking, switching, and unstacking have been successfully demonstrated on a four-node hubbed ring network serving five source–destination pairs on four wavelengths. Each wavelength was running at 1-Gb/s bit rate.

Index Terms—Fiber-optics communications, multiplexing, optical networks, packet switching, photonic slot routing, wavelength-division multiplexing (WDM).

I. INTRODUCTION

FUTURE GENERATIONS of metropolitan networks will have to cope with bursty data traffic with rapidly changing patterns. They will also have to be bit-rate scalable in order to accommodate the possibility of bandwidth demand growth. Packet-switched networks have a potential to satisfy all these requirements. However, while telecommunication networks are evolving toward packet switching, wavelength-division-multiplexing (WDM) systems still remain circuit switched since fast wavelength tunability of network components is both a challenge and the key to true packet-switched WDM networks. Tunable lasers open the possibility to connect to any WDM node with a single transmitter, thus enhancing network flexibility and enabling smooth network upgrades. To extract the utmost from a reconfigurable network, one would need not only tunable transmitters, but also tunable wavelength add–drop multiplexers (WADM). Such networks are sometimes referred to as tunable transmitter–tunable receiver (TTTR) networks. While both tunable lasers with nanosecond wavelength tuning speed and fast wavelength-insensitive optical switches with gigahertz responses are becoming available, currently there seems to be no cost-effective way to reconfigure wavelength add–drop multiplexers adequately fast. Therefore, one is restricted to network architectures with fixed or slowly reconfigurable receivers or networks employing power-splitter-based packet insertion [1], [2]. This approach makes it difficult to

change the bandwidth allocation in response to changes in the traffic pattern.

In this paper, we describe the first experimental demonstration of a highly connected and fully reconfigurable composite-packet-switched hubbed ring network. Packet switching in our network is done using fast polarization-independent 2×2 electrooptic switches. The wavelength dimension is used for transport rate multiplication. While the proposed approach avoids the use of tunable WADMs, it can achieve the same capacity as a network with TTTRs [3]. These added benefits come at a certain cost: the known bandwidth allocation protocol does not guarantee the access time as short as in TTTR schemes.

II. SYSTEM ARCHITECTURE

Photonic slot routing, introduced by Chlamtac *et al.* [4], combines the features of both time-division multiplexing (TDM) and WDM to achieve extremely high connectivity and flexibility while at the same time addressing the limitations of existing photonic switching technologies. In the original proposal [4], packets filling the time slots are generated and dropped in subtending optical rings in a distributed manner. Each of the nodes on a subtending ring is equipped with a fixed wavelength drop, a tunable laser, and a power splitter. This approach promises high connectivity on a larger scale network [5], [6] but faces implementational challenges such as power budget limitation due to cumulative splitter insertion losses and synchronization problems both in the core and in subtending rings. We propose a ring photonic slot routing network in which composite packets are generated locally at each node with a single tunable transmitter. We begin the description of our system by first introducing the notions of composite packets and packet-stacking techniques.

The node architecture of our proposed network is shown in Fig. 1. A “composite optical packet” consists of a multiplicity of fixed-length packets multiplexed in wavelength and synchronized in a single time slot. Individual packets of length T_p are generated serially at different wavelengths $\lambda_1, \lambda_2, \lambda_3, \dots$ by a tunable laser source. These packets are sent to a wavelength stacker consisting of an optical circulator followed by fiber Bragg gratings (FBG) spaced by fixed optical delay lines $T_p/2$. As illustrated in Fig. 1, packets generated by the tunable laser go through an optical circulator C_1 and travel down the FBG string. Each FBG reflects a specific wavelength as indicated and is transparent to all other wavelengths. The order of the wavelengths reflected by FBGs is the reverse order of packet generation: each wavelength’s packet is reflected

Manuscript received October 18, 2002; revised March 19, 2003.

M. Boroditsky, N. J. Frigo, and A. Smiljanić are with the AT&T Laboratories, Middletown, NJ 07748 USA.

C. F. Lam is with the OpVista, Irvine, CA 92618 USA.

K. F. Dreyer is with the Lucent Technologies, Murray Hill, NJ 07974 USA.

D. A. Ackerman, J. E. Johnson, L. J. P. Ketelsen, and A. Chen are with Agere Systems, Berkeley Heights, NJ 07922 USA.

Digital Object Identifier 10.1109/JLT.2003.814928

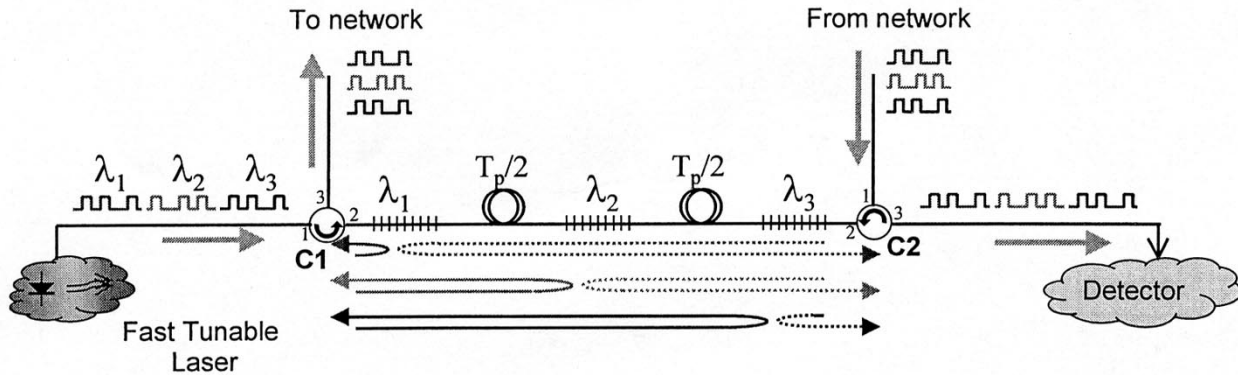


Fig. 1. Composite packet stacker/unstacker (S/U). A composite packet consists of several packets carried at different wavelengths and aligned in time. Composite packets are generated by passing packets of length T_p generated serially by a single tunable laser through a wavelength-dependent delay line. In our experiment, the wavelength-dependent delay line was realized using several FBGs and a circulator. Different wavelengths, generated at different times, experience different delays and will emerge from port 3 of the circulator C_1 synchronized in time, or stacked, to form a composite packet.

by its corresponding FBG and emerges from the third port of circulator C_1 . Thus the packet at wavelength λ_3 in Fig. 1 is generated first but will undergo the longest delay in the stacker. The packet at wavelength λ_2 is generated with a delay of T_p relative to the λ_3 packet, and the λ_2 packets experience T_p less delay in the stacker compared to λ_3 packets. Finally, the last packet is generated at wavelength λ_1 and experiences $2T_p$ less delay than the first packet at λ_3 . Consequently, the serial packets generated by the tunable distributed Bragg reflector (DBR) laser at different wavelengths are stacked into the same photonic time slot, forming a composite packet.

The same set of gratings can potentially be used to reserialize the stacked packet, as also shown in the right-hand side of Fig. 1 with dotted lines. The stacked signal enters Port 1 of the circulator C_2 , and the unstacked output emerges from port 3. Thus, a stacker and an unstacker provide serial-to-parallel and parallel-to-serial converters, respectively, by passive optical means. Alternatively, a wavelength-division multiplexer with optical delay lines can also be used for packet stacking. The cumulative loss in the stacking/unstacking using FBGs is $4L_C + 2WL_{\text{FBG}}$, where L_C is a circulator loss (in decibels), L_{FBG} is a loss in the grating, and W is the number of wavelengths. If the arrayed-waveguide grating (AWG) solution is used, then the loss for stacking and unstacking becomes $4L_C + 4L_{\text{AWG}}$, where L_{AWG} is the loss in the AWG and is independent of the number of wavelengths. For small W , as in our experiment with $W = 4$, FBGs are preferred, but for large wavelength count, when $W > 2L_{\text{AWG}}/L_{\text{FBG}}$, AWGs are advantageous.

The system architecture is shown schematically in Fig. 2. As shown before, the composite packets emerge from the third port of C_1 , which is connected to the ring network through a 2×2 polarization- and wavelength-insensitive optical switch (as shown in Fig. 2). The 2×2 wavelength-insensitive crossbar switches at each node can add/drop composite packets into/from the ring network or pass them through the node. One can see that in our approach the wavelength dimension is used for transport bit-rate multiplication, rather than for addressing different users, although wavelength routing still can be applied to the composite packets removed from the network [7]. Since the packets are routed on a time-slot basis, users at each node can

send packets to users at any other node by creating a composite packet that is inserted at the time slot at which the destination node will drop. This two-dimensional multiplexing technique in both wavelength and time domains can significantly enhance the network connectivity.

From the higher level network perspective, the transport rate multiplication achieved by passive optical means is identical to using faster transmitters and receivers. However, optical multiplexing offers better scalability: for example, using 16 wavelengths increases the transport rate by a factor of 16 in a straightforward manner. However, a sixteenfold increase of the speed of electronics needed to achieve the same effect is quite challenging.

Synchronization is a common problem for closed optical packet rings: as the circumference of the fiber plant changes with temperature, the length has to be constantly readjusted to correspond to an integral number of time slots. Hubbed rings, in which signals are regenerated in one of the nodes, are widely used, so that optical/electrical/optical (O/E/O) conversion removes the timing issues, and the optical part is essentially a bus. In the following, we do not address the synchronization issue.

An out-of-band control channel is necessary for building a real network. Such a channel could be terminated and regenerated at every node, e.g., as proposed in [2]. The network control is simplified since the load is balanced over the wavelengths at the physical layer. On the other hand, the control algorithm has to handle restrictions due to the fact that transmission and reception at any given node has to occur once per W time slots. We proposed (but did not implement) a new credit-based medium access control (MAC) protocol, utilizing discretely tunable delay lines, which features both good capacity utilization and simple admission control [3]. It has been shown in [3] that the admission control algorithm requires only minimal processing complexity while, at the same time, it has the ability to quickly react to typical traffic changes in data networks. The utilized switching capacity is the same as in networks where users are equipped with fast tunable lasers and fast tunable filters. However, even without tunable delay lines the same switching capacity can be achieved by using two fast tunable lasers per node.

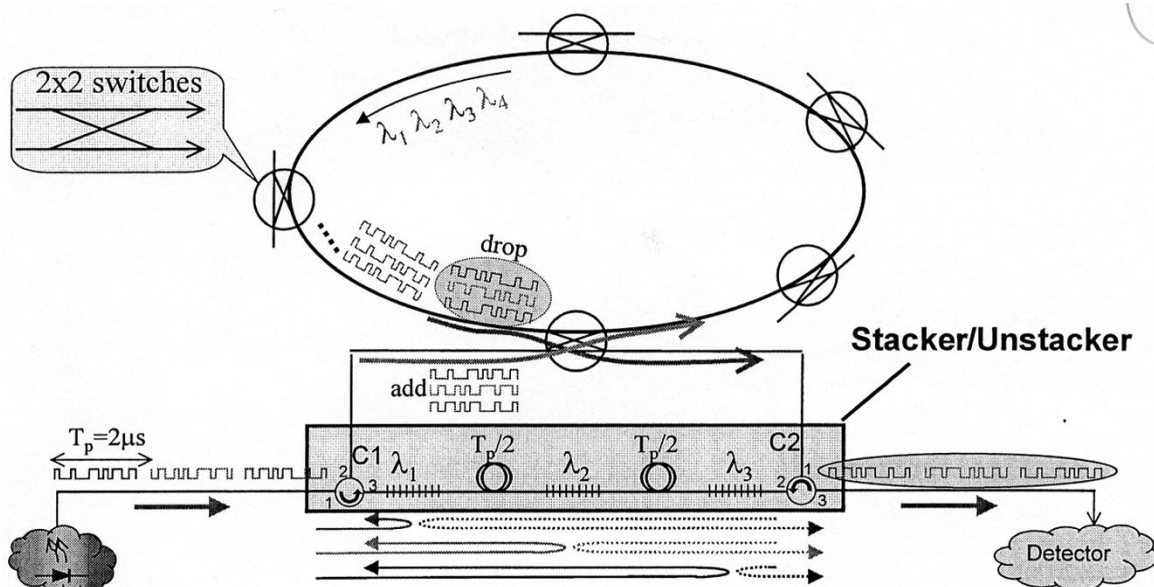


Fig. 2. Composite-packet photonic slot routing architecture. The composite packet can be added to or dropped from the ring by setting the wavelength-insensitive 2×2 optical switch into the “cross” position.

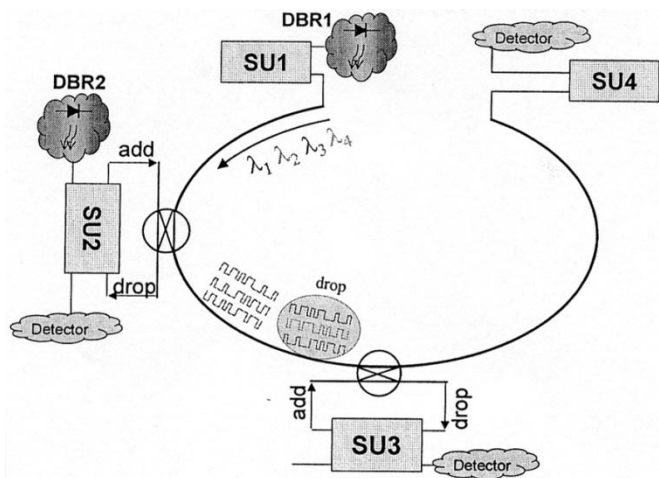


Fig. 3. Four-node experimental composite packet-switched network setup. Node 1 generates composite packets, node 2 receives and generates composite packets, and node 3 and node 4 only receive composite packets.

Similar to [3], the time is divided into cycles of W time slots. In each cycle, a node transmits at most one composite packet, and at most one composite packet is transmitted to any receiver. Nodes announce the packets that they will transmit two cycles in advance on a separate control channel. Because wavelength stacking of a packet lasts one cycle, the stacking of composite packets in two subsequent cycles might overlap if the packet in the earlier cycle is to be transmitted in the later time slot. Therefore, each node has to be equipped with two fast tunable lasers that are connected to a stacker through a coupler and that transmit composite packets in subsequent cycles. A 2×2 optical switch at the receiving node will drop a composite packet exactly two cycles after the node has recognized its address on the control channel. One of two detectors will receive the composite packet in question, while the other detector will receive the composite packet in the next cycle if the one arrives.

Packet alignment in a composite packet can be affected by chromatic dispersion in large networks. Nevertheless, a simple calculation shows that in a 50-km circumference ring using standard single-mode fiber (SMF), the maximum composite packet spread is about 10 ns if 16 channels with 100-GHz spacing are used. This is comparable with the switching time of the tunable lasers and optical switches and is much shorter than a packet length. To maintain the composite packet synchronization in a larger scale network, span-by-span chromatic dispersion compensation can be used, or the FBGs could be preskewed at a slight penalty in guard band.

III. EXPERIMENT AND RESULTS

To explore the feasibility of our proposed architecture beyond the concept demonstration [7], we built a 15-km circumference four-node demonstration network operating on four wavelengths, as shown in Fig. 3. Each node contains a four-wavelength stacker/unstacker (SU) unit with 100-GHz wavelength spacing. Wavelength- and polarization-independent 2×2 LiNbO₃ switches [8] at nodes 2 and 3 are used to route composite packets, as shown in Fig. 2. The switch drivers used in our experiment limit our switching time to about 20 ns. Node 1 generates composite packets destined for nodes 2, 3, and 4. Node 2 drops packets from node 1 and adds (or passes through) composite packets for nodes 3 and 4. Node 3 drops packets from both node 1 and node 2 and passes the composite packets for node 4. In this way, the network serves five source–destination pairs. Adjacent FBGs in all four S/U are separated by 200 m, corresponding to a time slot of about 2 μ s.

We used tunable DBR lasers with monolithically integrated semiconductor amplifiers and 2.5-Gb/s electroabsorption modulators (EAMs) [9], each packaged with high-speed electrical connections to both the tuning and modulator sections. The DBR laser wavelengths are discretely switched in less than 5 ns on a comb of four wavelengths spaced by 100 GHz. The

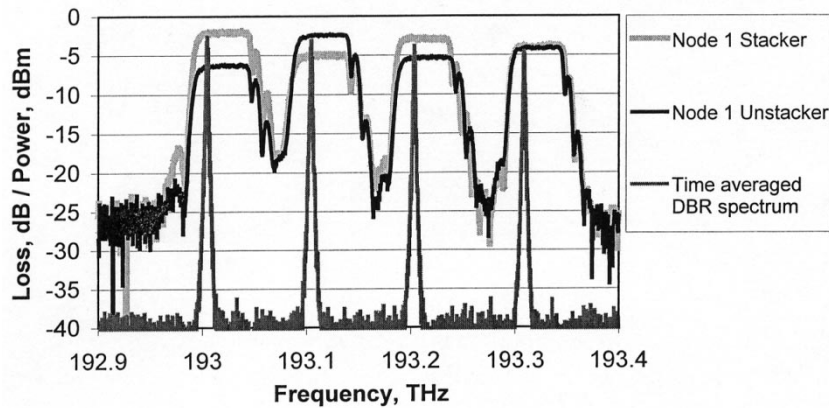


Fig. 4. Spectral responses of the stacker at node 1, unstacker at node 2, and the time-averaged tunable DBR laser output spectrum at node 1. The tunable laser hops between four channels, spaced by 100 GHz, and its output is suppressed during wavelength transitions time, which is less than 10 ns.

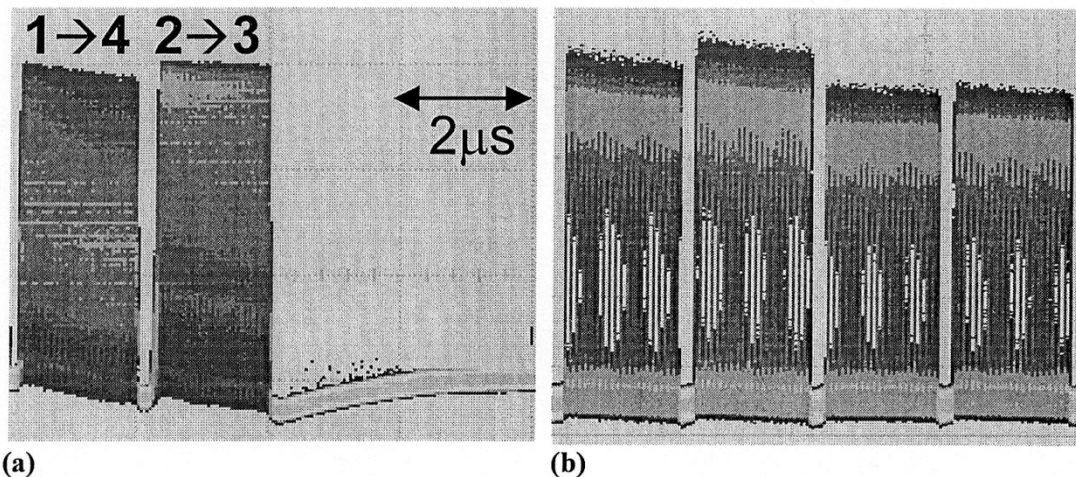


Fig. 5. Scope traces of the optical packet data. Trace 1 is taken on the link between nodes 2 and 3. It shows two stacked composite packets. One goes from node 1 to node 4, and the other goes from node 2 to node 3. Trace 2 demonstrates successful unstacking of a composite packet dropped by a 2×2 switch at node 3. The horizontal scale is $2 \mu\text{s}/\text{div}$.

wavelength comb can be fine-tuned as a unit by changing the laser temperature. Together with stackers, the DBR lasers at nodes 1 and 2 generate the composite packets. The two flat-top curves in Fig. 4 show the matching between the spectral response of the stacker and the unstacker. Fig. 4 also shows the time-averaged output power of a tunable DBR laser. The insertion loss in the stacker increases as the distance of the FBG from the circulator increases. On the other hand, the corresponding unstacker loss decreases in a complementary manner since the distance of its FBG from the second circulator increases. Thus stacking and unstacking losses tend to balance each other out in the overall system. The stacked composite packets from node 1 are transmitted through a 5-km-long SMF to node 2, which drops every third composite packet from node 1 and adds its own composite packets into the ring. The packets dropped at nodes 2, 3, and 4 are unstacked and recovered serially at all four wavelengths using an avalanche photodiodes (APD) detector, as will be shown subsequently.

An arbitrary waveform generator is programmed for the wavelength tuning of our DBR lasers. In order to minimize transients during wavelength switching, the order of the

switching was such that all frequency jumps were no more than 200 GHz ($1- \rightarrow 3- \rightarrow 4- \rightarrow 2- \rightarrow 1$). The serial packet data at the 1-Gb/s bit rate are generated by a multi-channel parallel bit-error-rate test set synchronized to the wavelength tuning voltage and applied to the EAM section of each DBR laser. Two polarization-independent 2×2 LiNbO₃ optical switches at nodes 2 and 3 are also driven by the same test set. A 7808-b (976-B) composite packet consisting of 7648 random b and 160-b guard time was used as the input signal. This corresponds to a time slot duration of approximately $2 \mu\text{s}$ and 98% bandwidth utilization with our synchronized system. During the guard time, the laser output is turned off using the built-in EAM to avoid spurious output at intermediate wavelengths caused by wavelength transitions. The guard time also allows for timing jitter produced by mismatches in the fiber delay lines between the FBGs. For the purpose of this experiment, a centralized clock (clock stratum) was used. However, with the use of burst-mode receivers that can sync in with only a 4-b training sequence [10], bandwidth utilization numbers will not change significantly. Trace (a) of Fig. 5 shows the signal on the link between nodes 2 and 3. It shows two consecutive stacked

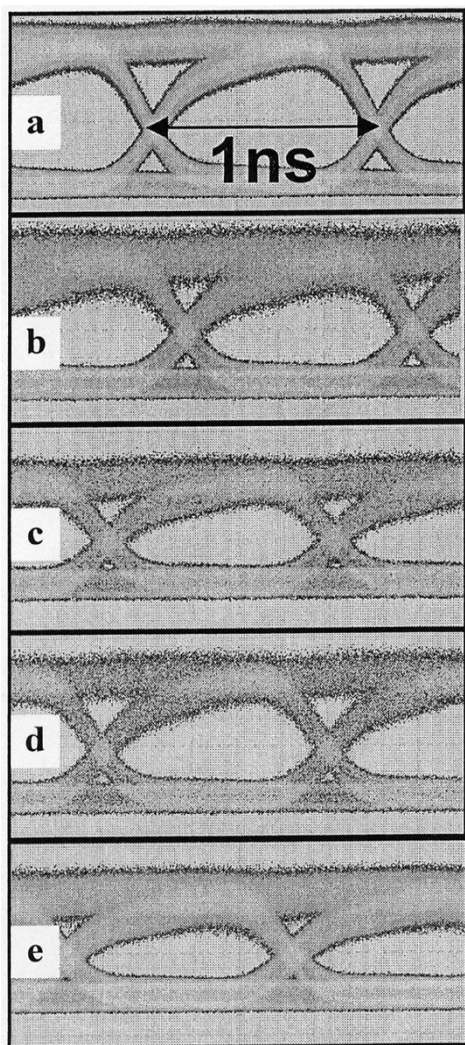


Fig. 6. Eye diagrams at 1 Gb/s of (a) the input packets at node 1, and (b)–(e) recovered individual wavelength packets at node 3. The horizontal scale is 0.4 ns/div.

composite packets, of which one is generated at node 1 for node 4, and the other is generated at node 2 for node 3. The stacked signals on all four wavelengths are detected simultaneously by an optical receiver. Individual wavelengths are well aligned within the $2 \mu\text{s}$ time slots as indicated, showing successful stacking.

Composite packets switched out of the network are optically amplified with a low noise optical preamplifier and reserialized (i.e., unstacked) at the output of nodes 2–4. Four unstacked components of a composite packet are shown in Trace (b) of Fig. 5. In this trace, every spectral component of the composite packet is detected separately. The dropped packets at all four wavelengths were successfully recovered using an APD detector. Fig. 6 shows the typical eye diagram of the input packets [Trace (a)] and those of the demultiplexed packets at each individual wavelength [Traces (b)–(e)]. The eye diagrams clearly demonstrate successful data recovery after the unstacking process.

The S/U used in our experiment is based on FBG technology (see Fig. 1), and its design is similar to that of an FBG add-drop

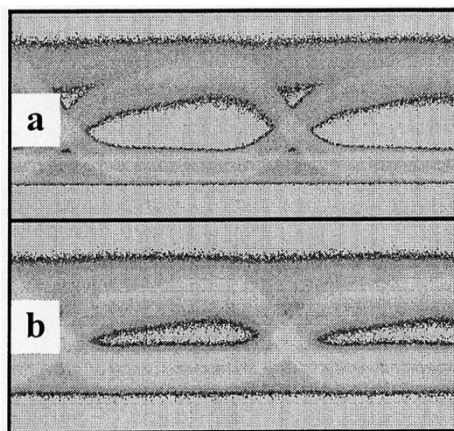


Fig. 7. Eye closure due to the crosstalk in the S/U [Trace (a)], which can be avoided [Trace (b)] by separating add and drop functions in time or by physically separating stacker and unstacker.

multiplexer. These components can cause crosstalk due to the leakage of the optical signal from the input port into the output port [11]. In Fig. 7, the Trace (a) of the output signal was detected in the absence of the input signal, while the signal in Trace (b) was detected in the presence of the crosstalk. In the current implementation, the crosstalk impairments were avoided by choosing a schedule such that adding and dropping of composite packets occurs in different time slots for any given node. However, using components with better optical rejection, or physically separated stackers and unstackers, will solve this problem as well.

IV. CONCLUSION

In conclusion, we proposed and successfully demonstrated a novel high-connectivity composite-packet-switching system using a single tunable laser source and passive optical components at each node to stack and unstack composite packets. Three key components of the proposed network—stacking, switching, and unstacking—were demonstrated in a four-node network operating at four wavelengths and serving five source-destination nodes operating with a synchronized clock.

The results presented here are readily scalable to higher (up to a 16) wavelength count and to 10-Gb/s transmitter line rates by using existing tunable lasers and with commercially available switches and AWGs. The proposed system is bit-rate-independent as long as the packet duration, defined by the lengths of the delay lines, remains unchanged. The usefulness of the composite packet switching in practice will be defined by developments in the field of optoelectronics. In particular, the applicability of composite packet switching will depend on the unavailability of fast tunable filters, and on the availability of either variable optical buffers or the creation of an efficient MAC protocol that does not require switchable delay lines. In certain circumstances, composite packet switching can not only become an economical solution for Internet protocol networks which require high connectivity and packet switching such as local area networks, but also could be an economically viable solution for interconnecting large router farms (i.e., operating as a distributed high-capacity switch).

ACKNOWLEDGMENT

The authors wish to thank Prof. E. Yablonovitch of the University of California, Los Angeles (UCLA), for lending us the necessary pieces of equipment, and A. Smiljanić for developing media access protocol and bandwidth allocation in composite-packet-switched networks.

REFERENCES

- [1] M. A. Marsan, A. Bianco, E. Leonardi, A. Morabito, and F. Neri, "All-optical WDM multi-rings with differentiated QoS," *IEEE Commun. Mag.*, vol. 37, pp. 58–66, Feb. 1999.
- [2] I. M. White, M. S. Rogge, Y.-L. Hsueh, K. Shrikande, and L. G. Kazovsky, "Experimental demonstration of the HORNET survivable bi-directional architecture," in *Proc. Optical Fiber Communication Conf. (OFC)*, vol. 70, 2002, pp. 346–349.
- [3] A. Smiljanić, M. Boroditsky, and N. J. Frigo, "High-capacity packet-switched ring network," *IEEE Commun. Lett.*, vol. 6, pp. 111–113, Mar. 2002.
- [4] I. Chlamtac, V. Elek, A. Fumagalli, and C. Szabo, "Scalable WDM access network based on photonic slot routing," *IEEE/ACM Trans. Networking*, vol. 7, pp. 1–9, Feb. 1999.
- [5] H. Zang, J. P. Jue, and B. Mukherjee, "Capacity allocation and contention resolution in a photonic slot routing all-optical WDM mesh network," *J. Lightwave Technol.*, vol. 18, pp. 1728–1741, Dec. 2000.
- [6] V. Elek, A. Fumagalli, and G. Wedzinga, "Photonic slot routing: A cost-effective approach to designing all-optical access and metro networks," *IEEE Commun. Mag.*, vol. 39, pp. 164–172, Nov. 2001.
- [7] M. Boroditsky, C. Lam, A. Smiljanić, M. Feuer, S. Woodward, K. F. Dreyer, D. A. Ackerman, J. E. Johnson, and L. J. P. Ketelsen, "Experimental demonstration of composite packet switching on a WDM photonic slot routing network," in *Proc. OFC'2001*, Anaheim, CA, 2001, Paper ThG6 (v. 4).
- [8] A. Chen *et al.*, "High performance LiNbO₃ switches for multi-wavelength optical networks," in *Photonics in Switching Conf., OSA Tech. Dig.*, 1999, pp. 113–115.
- [9] L. J. P. Ketelsen *et al.*, "2.5 Gb/s transmission over 680 km using a fully stabilized 20 channel DBR laser with monolithically integrated semiconductor optical amplifier, photodetector, and electroabsorption modulator," presented at the OFC 2000, Baltimore, MD, Postdeadline Paper D14.
- [10] Y. Ota, R. G. Swartz, V. D. Archer III, S. K. Korotky, M. Banu, and S. E. Dunlop, "High-speed, burst-mode, packet-capable optical receiver and instantaneous clock recovery for optical bus operation," *J. Lightwave Technol.*, vol. 12, pp. 325–331, Feb. 1994.
- [11] M. Boroditsky, C. F. Lam, M. D. Feuer, S. L. Woodward, and N. J. Frigo, "Enhancement of passive optical ring system performance by power management," *Electron. Lett.*, vol. 37, no. 6, pp. 1236–1238, 2001.

Misha Boroditsky, photograph and biography not available at the time of publication.

Nicholas J. Frigo (S'76–M'80), photograph and biography not available at the time of publication.

Cedric F. Lam (S'91–M'99), photograph and biography not available at the time of publication.

Kevin F. Dreyer, photograph and biography not available at the time of publication.

David A. Ackerman (M'95), photograph and biography not available at the time of publication.

John E. Johnson (S'82–M'84), photograph and biography not available at the time of publication.

Leonard J. P. Ketelsen, photograph and biography not available at the time of publication.

Antao Chen, photograph and biography not available at the time of publication.

Aleksandra Smiljanić, photograph and biography not available at the time of publication.